

## Supporting Information

### Stable Ni Nanocrystals on Porous Single-Crystalline MgO particles for Enhanced Dry Reforming Activity and Durability of CH<sub>4</sub>/CO<sub>2</sub>

Suning Zhang,<sup>ab</sup> Fangyuan Cheng<sup>\*abc</sup> and Kui Xie<sup>\*abc</sup>

<sup>a</sup> College of Chemistry, Fuzhou University, Fuzhou 350108, Fujian, China.

<sup>b</sup> Key Laboratory of Design & Assembly of Functional Nanostructures, Fujian Institute of Research on the Structure of Matter, Chinese Academy of Sciences, Fuzhou 350002, China.

<sup>c</sup> Fujian Science & Technology Innovation Laboratory for Optoelectronic Information of China, Fuzhou, Fujian 350108, China.

\* Corresponding author: [cfy@fjirsm.ac.cn](mailto:cfy@fjirsm.ac.cn) (F. Cheng), [kxie@fjirsm.ac.cn](mailto:kxie@fjirsm.ac.cn) (K. Xie).

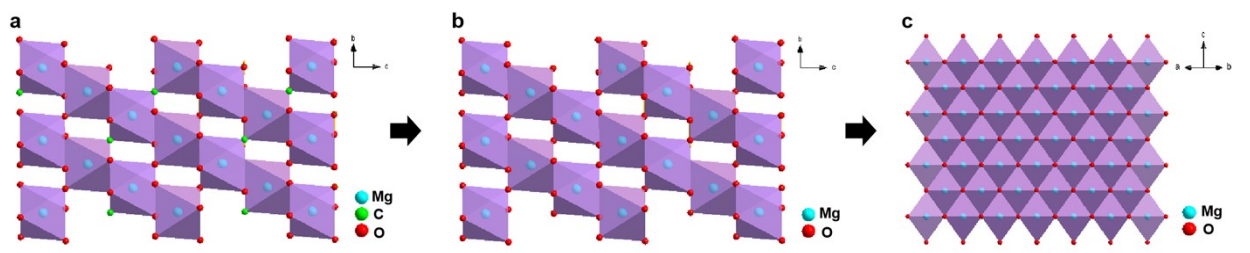


**Figure S1.** (a-c) The growth diagram from SC MgCO<sub>3</sub> particles to PSC MgO particles using the lattice reconstruction strategy.

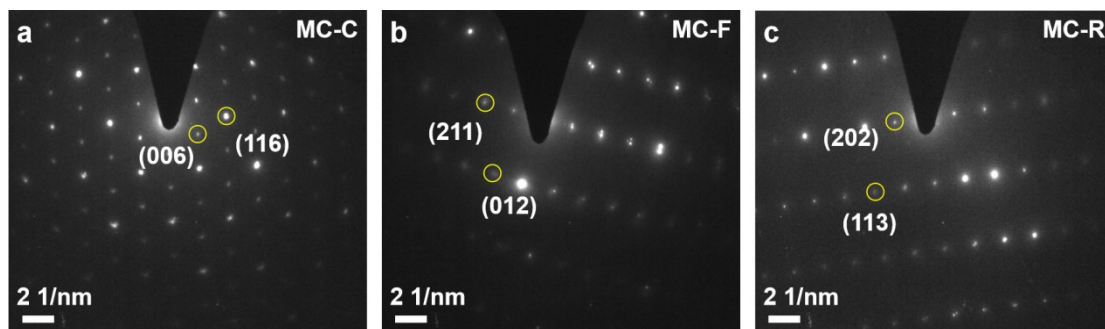


**Figure S2.** (a-c) SAED patterns of MC-C, MC-F and MC-R.

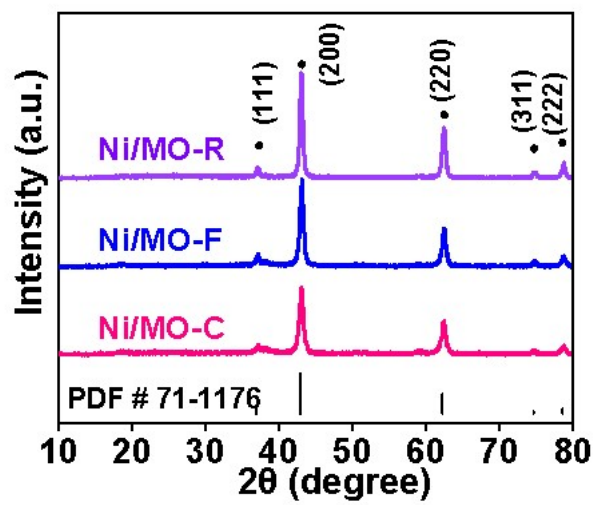


**Figure S3.** XRD patterns of PSC Ni/MgO particles.

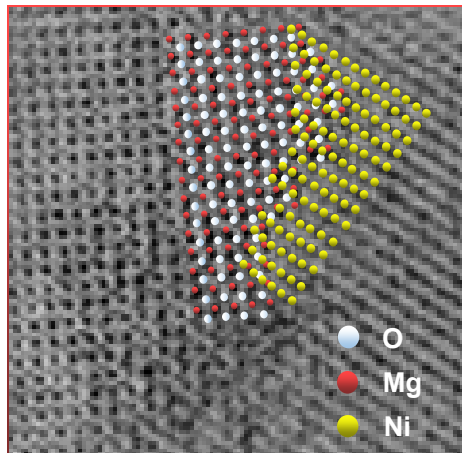


**Figure S4.** HR-TEM image of PSC Ni/MgO with well-defined interface structure.

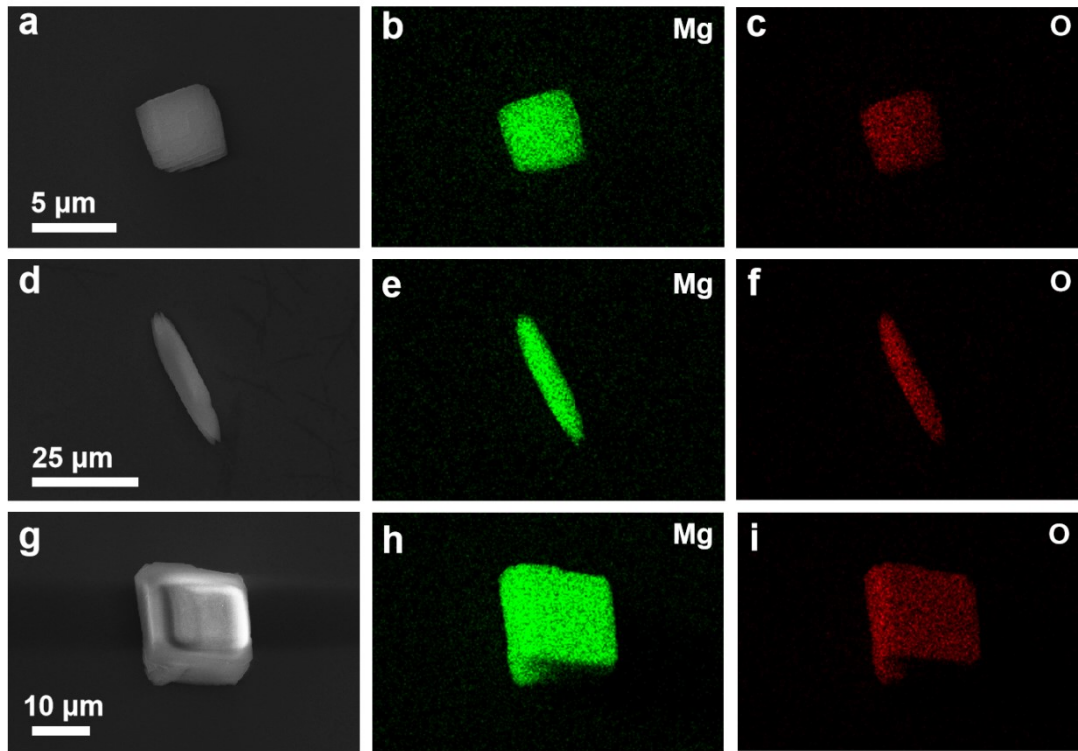
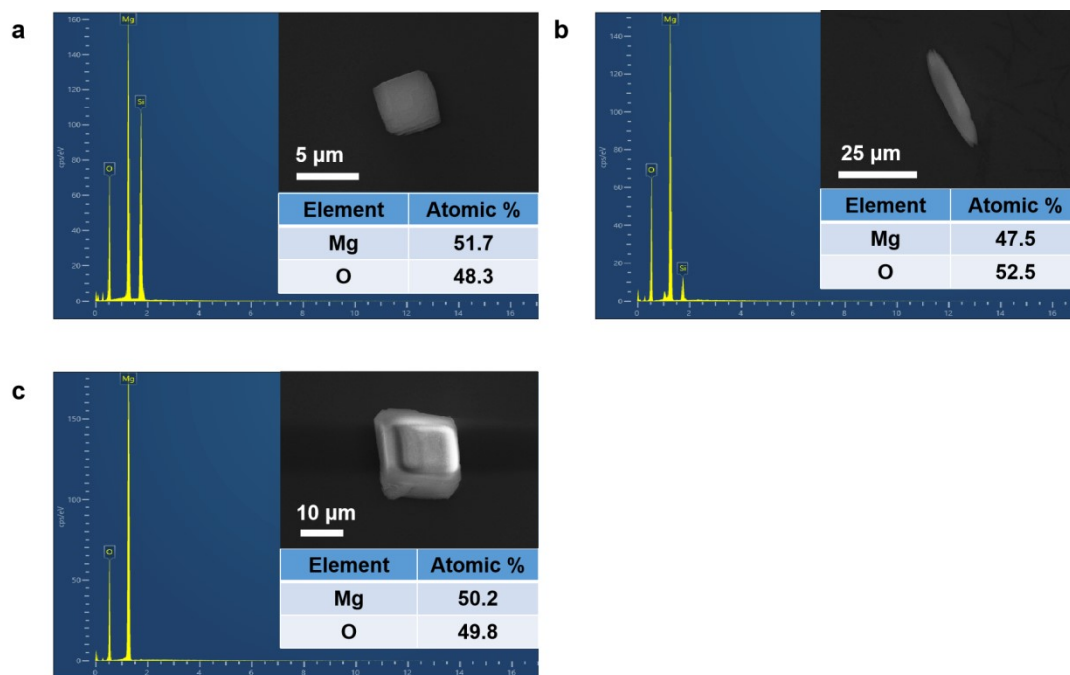
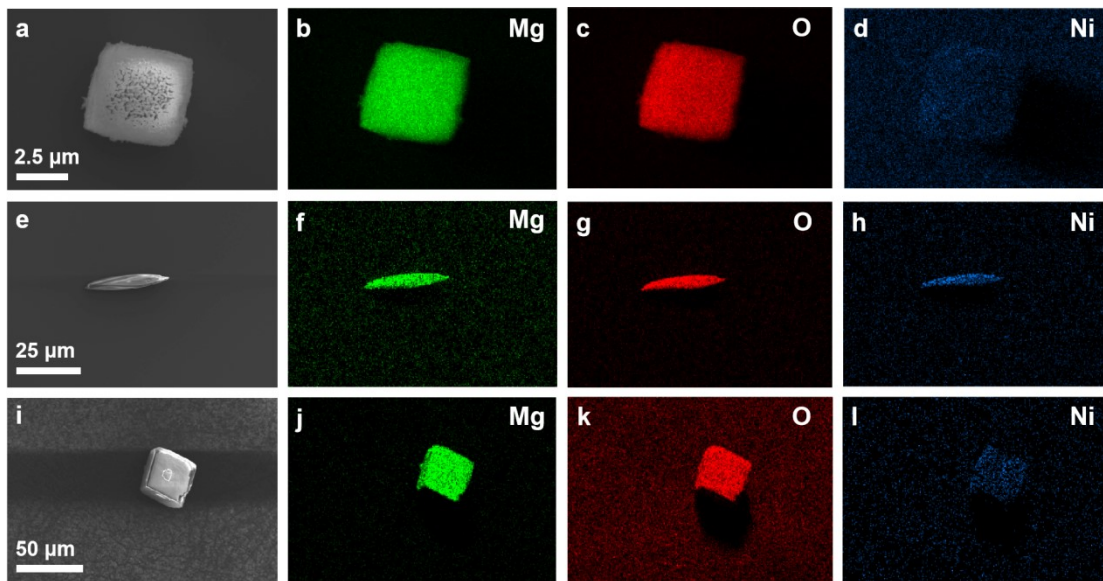


Figure S5. (a-i) Element mappings of PSC MgO particles.



**Figure S6. (a-c)** EDS test of PSC MgO particles with different morphology.



**Figure S7.** (a-l) Element mappings of PSC Ni/MgO particles.



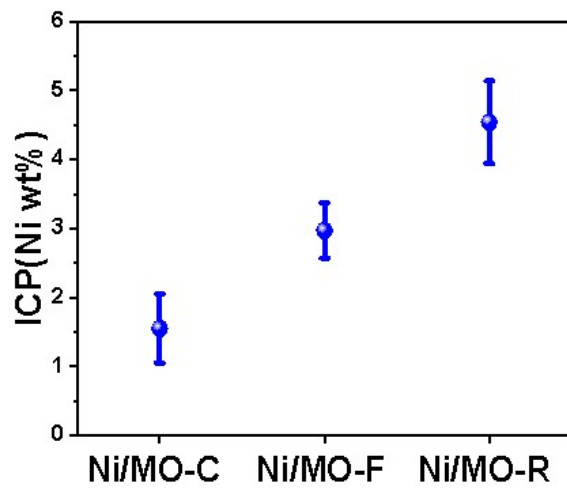


**Figure S8.** PSC Ni/MgO load with different SC Ni nanoparticle contents.

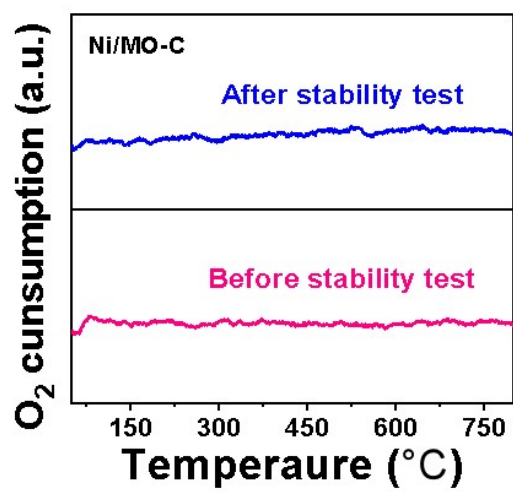


**Figure S9.** The TPO profiles of PSC Ni/MgO before and after 150 hours of DRM long-term testing at 700 °C.

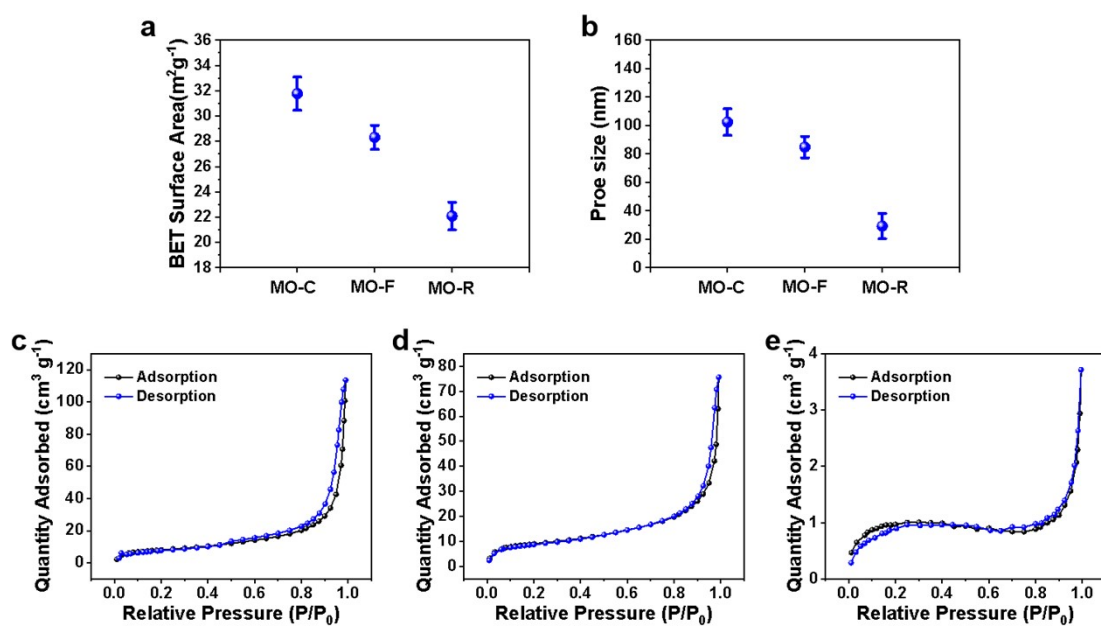


**Figure S10.** (a-b) BET surface area and BJH average pore size of PSC MgO with different morphologies. (c-e) N<sub>2</sub> adsorption-desorption isotherms of MO-C, MO-F, MO-R.

**Table S1.** The comparison of the performance of dry reforming of CO<sub>2</sub>/CH<sub>4</sub> under typical operation conditions.

Catalyst	Gas composition	WHSV (L·g <sub>cat</sub> <sup>-1</sup> ·h <sup>-1</sup> )	Temperature	test time	CH <sub>4</sub> Conversion	CO <sub>2</sub> Conversion	H <sub>2</sub> /CO ratio	Ref
Ni/SiO <sub>2</sub> @Al <sub>2</sub> O <sub>3</sub>	CH <sub>4</sub> /CO <sub>2</sub> /N <sub>2</sub> = 1:1:0.2	12	800 °C	100h	62.8%	82.3%	0.82	[1]
Ni/MgO-SiO <sub>2</sub>	CH <sub>4</sub> /CO <sub>2</sub> /Ar= 1:1:1	18	700 °C	50h	88%	92%	0.75	[2]
NiMo/MgO	CH <sub>4</sub> /CO <sub>2</sub> /Ar= 1:1:8	60	800 °C	850h	100%	100%	1	[3]
Ni <sub>3</sub> GaC <sub>0.25</sub>	CH <sub>4</sub> /CO <sub>2</sub> /N <sub>2</sub> = 1:1:1	54	600 °C	72h	48%	52%	-	[4]
Ni/MgO	CH <sub>4</sub> /CO <sub>2</sub> /Ar= 1:1:2	80	800 °C	40h	72%	-	0.84	[5]
Ni/MgO-ZrO <sub>2</sub>	CH <sub>4</sub> /CO <sub>2</sub> =1:1 .2	60	800 °C	50h	90.5%	-	1.6	[6]
Ni/MgO (M-1)	CH <sub>4</sub> /CO <sub>2</sub> /Ar= 1:1:8	24	700 °C	150h	≥95%	≥96%	0.99	This work
Ni/MgO (M-2)	CH <sub>4</sub> /CO <sub>2</sub> /Ar= 1:1:8	24	700 °C	150h	≥90%	≥92%	0.96	This work
Ni/MgO (M-3)	CH <sub>4</sub> /CO <sub>2</sub> /Ar= 1:1:8	24	700 °C	150h	≥81%	≥89%	0.92	This work

## References

- [1]. J. W. Han, J. S. Park, M. S. Choi and H. Lee, *Applied Catalysis B: Environmental*, 2017, 203, 625-632.
- [2]. Q. Zhang, X. Feng, J. Liu, L. Zhao, X. Song, P. Zhang and L. Gao, *International Journal of Hydrogen Energy*, 2018, 43, 11056-11068.
- [3]. Y. Song, E. Ozdemir, S. Ramesh, A. Adishev, S. Subramanian, A. Harale, M. Albuali, B. A. Fadhel, A. Jamal and D. Moon, *Science*, 2020, 367, 777-781.
- [4]. K. Y. Kim, J. H. Lee, H. Lee, W. Y. Noh, E. H. Kim, E. C. Ra, S. K. Kim, K. An and J. S. Lee, *ACS Catalysis*, 2021, 11, 11091-11102.
- [5]. Y. Fu, W. Kong, B. Pan, C. Yuan, S. Li, H. Zhu and J. Zhang, *Journal of the Energy Institute*, 2022, 105, 214-220.
- [6]. B.-J. Kim, H.-R. Park, Y.-L. Lee, S.-Y. Ahn, K.-J. Kim, G.-R. Hong and H.-S. Roh, *Journal of CO<sub>2</sub> Utilization*, 2023, 68.